OPTICA

Free-space coupled superconducting nanowire single-photon detector with low dark counts

Andrew S. Mueller,[1,2,*] Boris Korzh,[2,5] Marcus Runyan,[2] Emma E. Wollman,[2] Andrew D. Beyer,[2] Jason P. Allmaras,[1,2] Angel E. Velasco,[2] Ioana Craiciu,[2] Bruce Bumble,[2] Ryan M. Briggs,[2] Lautaro Narvaez,[3] Cristián Peña,[3,4] Maria Spiropulu,[3] and Matthew D. Shaw[2]

[1]Applied Physics, California Institute of Technology, 1200 E California Blvd, Pasadena, California 91125, USA
[2]Jet Propulsion Laboratory, California Institute of Technology, 4800 Oak Grove Dr, Pasadena, California 91109, USA
[3]Division of Physics, Mathematics and Astronomy, California Institute of Technology, Pasadena, California 91125, USA
[4]Fermi National Accelerator Laboratory, Batavia, Illinois 60510, USA
[5]e-mail: bkorzh@jpl.caltech.edu
*Corresponding author: amueller@caltech.edu

Received 27 September 2021; revised 27 October 2021; accepted 31 October 2021; published 9 December 2021

A free-space coupled superconducting nanowire single-photon detector with high efficiency at 1550 nm, sub-0.1 Hz dark count rate, and sub-15 ps timing jitter is demonstrated.

https://doi.org/10.1364/OPTICA.444108

Time-resolved photon detection with low dark counts is a vital technology in fields such as quantum information processing, classical communication, quantum communication, and laser ranging. Increasingly, research in these fields employs superconducting nanowire single-photon detectors (SNSPDs), which have been demonstrated with system detection efficiency (SDE) (η) of more than 90% [1], timing jitter (Δt) as low as 2.6 ps [2], and intrinsic dark count rates (DCRs) (D) in the milli- to micro-hertz range [3]. However, quantum communication applications require detection systems with performance optimized across all three metrics simultaneously. The dimensionless figure of merit H specifies this application-specific performance as $H = \frac{\eta}{(\Delta t D)}$ [4].

Here, we focus on lowering the DCR of a telecom-band SNSPD system by filtering thermal photons, without sacrificing efficiency or jitter. We demonstrate a free-space coupled SNSPD with sub-0.1 Hz DCR, 14 ps timing jitter, and 72% total SDE by using a differential single-pixel SNSPD [5] to image a single-mode fiber through an optimized free-space filter stack.

The highest SDEs have been achieved using self-aligned fiber coupling where dark counts can be reduced using cryogenic fiber looping [6] or spliced narrowband filters [7]. But it is difficult to achieve strong filtering without losses at the target wavelength. Low-loss, high-rejection filters are typically available as free-space components, so some of the highest reported H-values were achieved with cryogenic, fiber to free space to fiber coupling, but exhibit an SDE of only a few percent [8]. The filtering method presented here takes advantage of commercially available filters, achieves a high free-space coupling efficiency using a cryogenic lens, and is compatible with both fiber and free-space optical inputs.

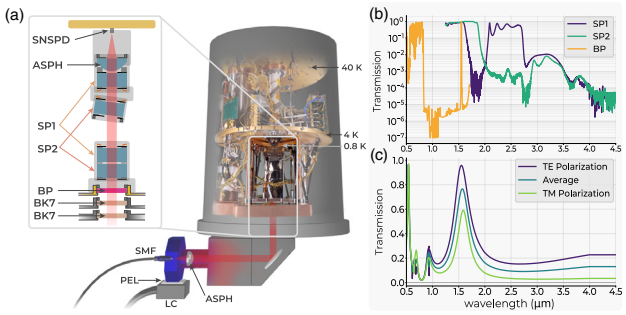

Fig. 1. (a) System hardware. ASPH, aspheric lens; SP1, SP2, custom short-pass filters; BP, bandpass filter; BK7, glass windows; SMF, single-mode fiber; PEL, Peltier element; LC, liquid cooling block. (b) Transmission spectra for the three filters utilized. (c) Absorption spectrum for the SNSPD efficiency-enhancing optical stack.

In this work, a single-mode fiber is imaged onto the detector using two $f = 18.75$ mm lenses. One lens collimates light from an optical fiber face outside the cryostat (Photon Spot), and the other focuses light onto the detector inside [9]. In the collimated region between, the beam passes though a series of short-pass filters and one bandpass filter mounted at 4 K [Fig. 1(a)]. One of the short-pass filters is angled to avoid ghosting effects. The 40 K radiation shield and outer cryostat housing are fitted with anti-reflection coated BK7 windows. The filters are spring loaded to prevent cracking at low temperatures. To minimize effects of stray light, the interior of the 4 K shield was painted with mid-IR absorbing paint (Aeroglaze Z306) [10], while gaps between filters and the windows were covered with metal tape.

The system is based on 1-inch (25.4 mm) optics, although the $f = 18.75$ mm lenses lead to a $1/e^2$ intensity diameter of about 5 mm in the collimated region. To reduce the larger-than-required numerical aperture of the system, painted 8 mm apertures (Acktar Spectral Black) were added in the collimated region. These are large

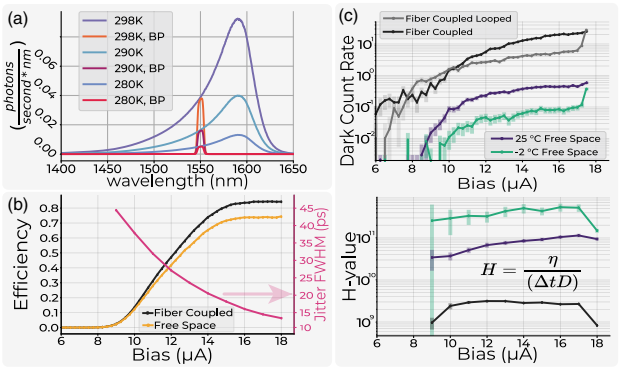

Fig. 2. (a) Simulated photon flux at various temperatures with and without the 1550 nm bandpass filter (BP). (b) Normalized photon count rate (PCR) and jitter measurements. (c) DCR, and calculated figure of merit H versus bias current for both fiber-coupled and free-space coupled configurations.

enough to allow minor alignment adjustments—by translating the exterior collimating lens—without vignetting.

We use four custom cryogenic short-pass filters, with passbands below 1.6 μm and 1.9 μm (Andover Corp.), both with transmission at 1550 nm of 98.8 ± 0.3%. They reject wavelengths shorter than 3 μm through reflective optical coatings, and attenuate longer wavelengths through material absorption in the 12.7-mm-thick N-BK7 glass substrate. While the bandpass filter (FWHM = 7 nm) was found to blueshift by about 2 nm at cryogenic temperatures, the passband was wide enough such that significant attenuation was not observed at the original target wavelength of 1550 nm. This filter is also sufficiently wide to avoid Fourier-limited broadening of ultra-short laser pulses.

The filtering of the optical stack was modeled by assuming a blackbody emitter at 298 K and a field of view defined by the 18.75 mm focal length of the cryogenic lens and the 8 mm diameter of the apertures. The resulting spectrum was multiplied by the transmission of the filters [Fig. 1(b)] and detector optical stack [Fig. 1(c)]. The model showed that two each of the 1.6 μm and 1.9 μm short-pass filters were necessary to suppress mid-IR light to where it was no longer the dominant source of dark counts. With the inclusion of the four short-pass filters, the dominant source of dark counts is the spectral region near 1550 nm as shown in Fig. 2(a), which also illustrates the effect of the bandpass filter. Also evident in Fig. 2(a) is the strong dependence of DCR on the temperature of the final surface outside the cryostat emitting thermal radiation. This motivated the exterior cooling apparatus shown at the bottom of Fig. 1(a). The bulkhead holding the fiber connector is cooled to around −2°C using a Peltier element and liquid cooling block. This addition reduced the system DCR from 0.4 Hz to below 0.1 Hz. While dark counts from multiple spatial modes are present in this system—modes that would not be present in a purely fiber based approach—the external cooling technique works to minimize their effect.

This work used a low-jitter, differential SNSPD [5], with an active area of 22 × 15 μm, formed by a meander of 100-nm-wide and 5-nm-thick niobium nitride (NbN) nanowires on a 500 nm pitch. A more conventional single-ended readout SNSPD of similar area would also achieve low DCR in this coupling system, but would likely achieve a lower performance metric H from correspondingly higher jitter. The nanowire is embedded in an efficiency-enhancing optical stack made of alternating layers of TiO_2 and SiO_2 and a gold mirror layer. As shown in Figs. 2(b) and 2(c), when fiber coupled (without any fiber-based filtering methods applied), this detector achieved a saturated SDE of 84% ± 4.4% and a DCR of 20 Hz at a bias current of 16 μA.

As also shown in Fig. 2(b), the free-space coupling system achieves up to 72% ± 3.7% SDE as measured from the fiber outside the cryostat. The reduction in efficiency is likely due to surface reflections in the free-space optics, and potential misalignment in the optical baffles. The minimum DCR [Fig. 2(c)] at 72% SDE is about 0.1 Hz, with a bias current of 16 μA. These metrics, with the jitter measurements shown in Fig. 2(b), give a maximum H-value of 5×10^{11} [Fig. 2(c)]. Values as high as 1.8×10^{12} have been reported before, but at 1.5% system detection efficiency [8]. Our system shows a low DCR can be achieved without severe reduction of SDE or usable target wavelength bandwidth. This is paramount for the future of terrestrial and space-to-ground quantum communication, since it increases the success rate with finite statistics [7]. The same techniques can be applied to emerging SNSPD applications at longer wavelengths, such as laser ranging [11], where fiber filtering is impractical. Beyond single-mode applications, our work paves the way to scalable, low-DCR, multi-mode coupling to SNSPD arrays [12].

Funding. Alliance for Quantum Technologies, California Institute of Technology; Jet Propulsion Laboratory; Defense Advanced Research Projects Agency; National Aeronautics and Space Administration (80NM0018D0004).

Acknowledgment. The research was carried out at the Jet Propulsion Laboratory, California Institute of Technology, under a contract with the National Aeronautics and Space Administration. We thank Jason Trevor for technical assistance and Sahil Patel for assisting in editing the paper. J.P.A. acknowledges a NASA NSTRF fellowship.

Disclosures. The authors declare no conflicts of interest.

Data Availability. The data that support the findings of this study are available from the corresponding author upon reasonable request.

REFERENCES

1. D. V. Reddy, R. R. Nerem, S. W. Nam, R. P. Mirin, and V. B. Verma, Optica **7**, 1649 (2020).
2. B. Korzh, Q. Y. Zhao, J. P. Allmaras, *et al.*, Nat. Photonics **14**, 250 (2020).
3. Y. Hochberg, I. Charaev, S.-W. Nam, V. Verma, M. Colangelo, and K. K. Berggren, Phys. Rev. Lett. **123**, 151802 (2019).
4. R. H. Hadfield, Nat. Photonics **3**, 696 (2009).
5. M. Colangelo, B. Korzh, J. P. Allmaras, *et al.*, "Impedance-matched differential superconducting nanowire detectors," arXiv:2108.07962 (2021).
6. J. D. Cohen, S. M. Meenehan, G. S. MacCabe, S. Gröblacher, A. H. Safavi-Naeini, F. Marsili, M. D. Shaw, and O. Painter, Nature **520**, 522 (2015).
7. A. Boaron, G. Boso, D. Rusca, C. Vulliez, C. Autebert, M. Caloz, M. Perrenoud, G. Gras, F. Bussières, M.-J. Li, D. Nolan, A. Martin, and H. Zbinden, Phys. Rev. Lett. **121**, 190502 (2018).
8. H. Shibata, K. Shimizu, H. Takesue, and Y. Tokura, Opt. Lett. **40**, 3428 (2015).
9. F. Bellei, A. P. Cartwright, A. N. McCaughan, A. E. Dane, F. Najafi, Q. Zhao, and K. K. Berggren, Opt. Express **24**, 3248 (2016).
10. M. J. Persky, Rev. Sci. Instrum. **70**, 2193 (1999).
11. G. G. Taylor, D. Morozov, N. R. Gemmell, K. Erotokritou, S. Miki, H. Terai, and R. H. Hadfield, Opt. Express **27**, 38147 (2019).
12. E. E. Wollman, V. B. Verma, A. E. Lita, W. H. Farr, M. D. Shaw, R. P. Mirin, and S. W. Nam, Opt. Express **27**, 35279 (2019).